Iris Recognition Scheme Based on Entropy and Convolutional Neural Network

Inass-Shahadha Hussein*, Noor-Abbood Jasim

Middle Technical University, Technical Institute of Baquba, Baghdad, Iraq

Received 28 March 2024; received in revised form 06 May 2024; accepted 07 May 2024

DOI: https://doi.org/10.46604/10.46604/aiti.2024.13516

Abstract

This study presents an advanced iris image segmentation approach to overcome vibration and occlusion from the lashes. The proposed scheme removes the surrounding areas of the iris image to recover the region of interest (ROI) containing the iris images. The entropy function and mathematical morphology are employed as the foundation of the proposed scheme. Initially, the entropy function is applied to the binarization image. Subsequently, the ROI is cropped and extracted from the binary image using the dilation method. Furthermore, a convolutional neural network (CNN) is used in the recognition phase. The database of the Indian Institute of Technology Delhi (IIT Delhi) serves as a test. The results yield a high level of accuracy—up to 93% during segmentation. Using half of the dataset during the recognition phase results in an accuracy of 98.8%, while using the complete database produces an accuracy of 97.5%.

Keywords: iris, segmentation, morphology, entropy, CNN

1. Introduction

Biometric technologies have evolved significantly, revolutionizing the field of identification and authentication. Initially, biometric methods were mainly correlated with fingerprints, and the earliest systems were developed in the late 1800s. However, as computing capacity and sensor technology have increased, the growth of biometric modalities, including voice, face, iris, and palmprint identification, etc., has ensued quantitatively [1].

Biometric identifications using the iris, sclera, and fingerprints have increasingly been employed for authentication [1]. Iris recognition (IR) has been habitually deployed in multifarious applications, e.g., security, e-commerce, finance, etc [2]. To discuss further, iris biometrics is the most accurate and safest method concerning identification. Additionally, among various physiological patterns, iris biometrics is well known for confidentiality and dependability [3]. However, a potential challenge lies in IR with the requirement for high-quality imaging devices and controlled environments to guarantee accurate and reliable results.

Mostofa et al. [4] have summarized the benefits of iris biometry, while the statements describe the iris as follows: (a) uniqueness: even if comparing a pair of irises of a certain person or twins, the irises are unreservedly heterogeneous; (b) stability: typically, iris develops from childhood and maintains the physical characteristics permanently; (c) the provision of texture information: iris furnishes the owner with texture information concerning stripes, spots, and coronas. (d) security: the iris is located in a circular area beneath the surface of the eye, between the black pupil and the white sclera. Hence, given the location, the iris is rarely affected externally. Meanwhile, with such a feature, faking the iris pattern is theoretically

* Corresponding author. E-mail address: inasshussin@mtu.edu.iq

English language proofreader: Chih-Wei Chang

impossible; (e) noncontact activation: Compared to biometrics undergoing tactile or any physical interaction, e.g., fingerprint recognition, IR is comparatively hygienic. Considering the aforementioned benefits, the iris has been employed in identification extensively.

Historically, the first automatic IR system was introduced by Daugman [5] in 1993. In this work, the iris region is first segmented using the conventional procedure in most IR works. Subsequently, from the segmented images, the desired features are retrieved. The majority of these characteristics are typically handcrafted. The use of manual features causes an impasse for traditional approaches. As a result, to resolve such developmental hindrance, Daugman [6] introduced the highly accurate and quick IR model in 2009, according to the Hamming distance and Gabor filter, and employed several iris datasets. On the other hand, pre-processing and segmentation are two requisite operations for the identification method, especially the initial step [7-8].

Technically, the intregro-differential operator and the Hough transform serve as the foundation for conventional iris segmentation techniques. Several algorithms employ variations to determine the iris borders of the Hough transform and the integro-differential operator. When iris images are captured in proper circumstances, these algorithms can accomplish adequate localization precision. The integro-differential operator, which is frequently employed during preprocessing, highlights pixel intensity variations to improve the edges of the iris. By identifying the borders, the operator assists in distinguishing the iris from adjacent components, such as the sclera and eyelids. After the edges are sharpened, the Hough transform is used to locate elliptical or circular shapes lining up with the edge of the iris. Hough transform is exceptionally effective at identifying parametric shapes, whose performance is evidenced when identifying the elliptical or circular iris boundary regardless of noise or occlusion. In contrast, however, if not fulfilling ideal conditions, noise will profusely be generated to interfere with the results of iris images, incurring a critical loss of accuracy concerning algorithm segmentation [2].

Iris segmentation utilizing the Hough transform and Daugman's algorithm was introduced by Rafik and Boubaker [9]. The authors of this study suggested calculating the iris and pupil radii sizes. Therefore, it is possible to trim the radius of the pupil (r1) and the radius of the iris (r2) for accurate segmentation. Daugman's algorithm presupposes the unique and high-quality patterns that lie in the iris images. Nevertheless, ambient brightness, motion blur, and occlusions (e.g., eyelids or lashes) can deteriorate image quality and cause errors in IR.

Additionally, Rapaka et al. [10] introduced a segmentation method for non-ideal iris images using morphology with fuzzy C-means (FCM) and dynamic spectrum access (DSA). However, similarly, environmental factors such as illumination, occlusions, image quality, etc., might further impact the accuracy of non-ideal iris images. Thus, in summary, efficacy in practical situations requires the operator to choose the approach properly according to the surrounding conditions.

In IR systems, deep learning, embodied by the convolutional neural network (CNN), has dominated computer vision research and has been envisaged to render remarkable effectiveness. Functionally, deep learning can automatically extract useful and feature representations from the image data, facilitating the optimization concerning the performance of IR techniques [3, 11]. Hence, IR techniques based on deep learning are being presented in the interim. Currently, manifold deep CNN models emerge in the existing literature, e.g., GoogleNet, AlexNet, residual neural network (ResNet), and visual geometry groups [9]. Table 1 summarizes the IR works based on deep learning.

Table 1 Related works based on deep learning

Author	Method	Database	Accuracy
Omran and AlShemmary [12]	IrisNet for extracting the attributes	IIT Delhi* V1	Original = 97.32% and normalized images = 96.43%
Alaslani and Elrefaei [13]	AlexNet model with support vector machine	IIT Delhi, CASIA 1.0 CASIA-V1, CASIA-Iris-V3	100%, 98.3%, 98%, 89%

Table 1 Related works based on deep learning (continued)

Author	Method	Database	Accuracy
Minaee and Abdolrashidi [14]	Residual CNN	IIT Delhi	95.5%
Wang et al. [15]	(MiCoRe-Net)	CASIAV4 and the UBIRIS.v2	99.08% and 96.12%
Azam and Rana [16]	CNN and SVM	CASIA	96.3%
Hsiao et al. [7]	U-Net and Efficient Net	CASIA v1	up to 98%.
Alwawi and Althabhawee [11]	CNN	Private	Training 95.33%, testing 100%
Balasubramanian et al. [3]	CNN	Multi dataset	Best accuracy 99.4%

*: Indian Institute of Technology Delhi (IIT Delhi)

As observed from the literature, segmentation becomes more challenging when there is vibration and occlusion from the lashes in the image. Therefore, this study introduces multifarious methods to segment the iris images and find the region of interest (ROI) of the iris while accounting for the unallocated feature in the images.

This study contributes to the technique for image improvement, which subsumes binarizing the image using the maximum entropy, calculating the image histogram entropy function, and using the median filter to reduce noise. Regarding binarization, this study used the histogram entropy information, which is the method extensively used for image thresholding. Compared to other methods, the generic nature of the algorithm affects the feasibility of using a global and objective property of the histogram. Subsequently, the iris dilates mathematically and separates from the desirable area of the images. As a result, the ROI can be recovered as expected. Specifically, dilation is used to identify the area within an image by progressively expanding the foreground pixel boundaries. To ensure the generation of details, the foreground pixels are enlarged while the holes within certain regions decrease.

Concerning the recognition, CNN is used. In multitudinous computer vision applications, such as image classification, object identification, and face recognition, CNN has shown unparalleled performance. Utilizing CNN architectures specifically designed for IR can conduce to improved accuracy and reliability [12]. Fig. 1 diagrammatically presents an illustration of the study.

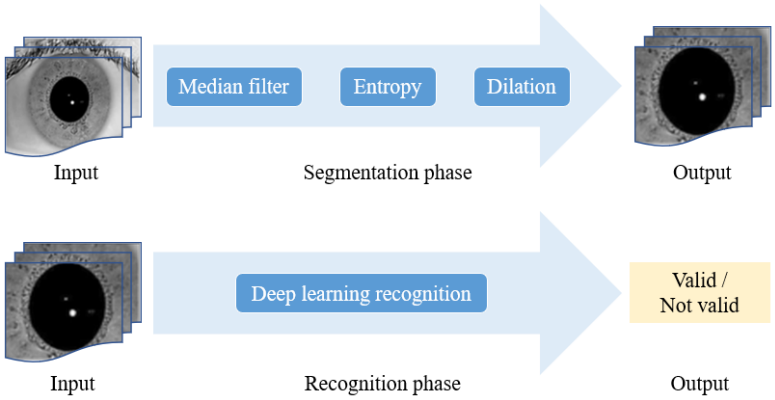

Fig. 1 Proposed study of iris recognition scheme

Synoptically, this paper enumerates the contents as follows. Section 2 introduces the materials and methods. Section 3 renders an elucidation of the recommended scheme, and Section 4 presents the experiment's findings. Eventually, the conclusion is drawn in Section 5.

2. Materials and Methods

This section introduces the materials and methods of the IR scheme used in this study in detail, including image histogram, median filter, entropy, and morphology, which are used in the segmentation phase. Meanwhile, the deep CNN structure used in the recognition phase is explained. Furthermore, the mathematical concepts for each method have been provided.

2.1. Image histogram

A histogram statistically represents the relationship between the pixel intensities and the frequency of occurrence of each intensity (0 to 255 in gray level) on the X-axis, which can be simply interpreted as the converse number of pixels on the Y-axis. A histogram in image processing delineates the relationship between two images concerning the intensities at a specific moment. As formulated below, the histogram is presented [17]. A histogram is widely used in image processing for thresholding and segmentation steps.

$$h(i) = g(i) \tag{1}$$

2.2. Median filter

The median filter is a straightforward nonlinear smoother, which can eliminate noise while retaining sharp, prolonged variations such as edges in signal values. Therefore, the median filter is evidenced by the ability to mitigate impulsive noise [18]. The median value of the central input data inside the window is the output of the filter at a certain moment. If the value $x(g)$ input image, while $y(g)$ output image. Meanwhile, both input and output of window size (2m + 1) are yielded with one-dimensional (1-D), and the output image after the median filter is given in:

$$y(g) = med\left\{x(g-m)\ldots, x(g)x(g-1)\ldots,(g+m)\right\} \tag{2}$$

where $1 \leq g \geq r$. Here, $x(1)$ and $x(r)$, while $r \in R$, are repeated (m) times at both the start and end of the input to account for startup and end impact.

2.3. Entropy function

In image processing, the measure of randomness or uncertainty in an image is measured by the entropy function. The entropy function measures the quantity of information or disorder in the pixel intensity distribution mathematically. Moreover, the entropy function is frequently employed as a criterion for choosing an ideal threshold value in image binarization, where the objective is to convert a grayscale image into a binary image, i.e., black and white only. According to the threshold value, pixels are dichotomously classed as black and white. Fundamentally, the concept entails determining the threshold and optimizing the entropy of the final binary image, which indicates that the threshold value is selected to produce a binary image with the maximum of information or randomness feasible. To determine the effectiveness, the results of separation between both foreground (items of interest) and background is proportional to entropy.

The binarization is to efficiently separate objects from the background and, simultaneously, retain information at best in the final binary image by maximizing entropy. Applications encompassing image processing, such as segmentation, optical character recognition (OCR), and object recognition, benefit greatly from binarization. The entropy function is presented:

$$En(h) = -\sum_{i=0}^{i=1} p_i \log p_i \tag{3}$$

2.4. Morphology

A cluster of methods, which is known as morphological operations, are used in image processing to structurally examine and modify an object according to topological and spatial properties. Morphological operations are useful for noise removal, feature extraction, object detection, and binary or grayscale images. Images are transformed based on shapes using morphology. An input image requires a scale factor application throughout morphological processes to generate an identically sized output image. The value of each output pixel from a morphological operation can be ascertained by juxtaposing the pixels in the input image [19]. The process is depicted in:

$$Z = z \times S \tag{4}$$

where Z is the new image, z is the image, and S is the scale factor (S > 0)

Alternatively, given that lengths are cognitively positive, the value of the scaling factor will be multiplied after rendering as a modulus. In the suggested study, dilation is to gradually enlarge the borders of the foreground pixel regions to identify a broad space in the images. Therefore, the area of foreground pixels expands while corresponding gaps are proximate to the features of the image [17]. Morphology preponderantly requires ascertaining available design models, whether existing or nascent, to establish the topological structure with certain specifications. Furthermore, this step purposively proceeds to opting several models for investigating the equivalent mechanism therein concerning the skeleton and kinematic chain. Consequently, new designs can be developed.

2.5. Convolutional neural network

An artificial intelligence class, which is also known as deep CNNs, can be used in sundry fields. Meanwhile, deep learning picks up features per se. Therefore, the primary objective is to enable a thorough comprehension of the material without requiring any manually created feature extraction [12].

CNN is typically employed in classification or image recognition. Historically, this method was created in the 1980s, whereas it was reintroduced in 2012. Currently, moreover, CNN is widely adopted in computer science. In addition to the presence of multiple hidden layers, CNN mimics the cerebral response by detecting visuals. By using several completely linked layers for classification and locally connected layers with automatic feature identification, CNN can automatically extract features [20]. Specialized neural network types comprise the extraction feature of neural networks based on weight updates and training. As stated above, CNN transforms the manual feature extraction processes into an automated system. Hence, each layer in CNN operates purposively and distinctly, while the network is composed of several layers [21].

The convolutional layer (convo) is a collection of learnable filters with a set of weights combined. The weight values were chosen at random and learned via the backpropagation approach. The features map, which filters the entire image with the learned weight [22], identifies the unique features in the initial input image and is calculated using the following,

$$z^S = F\left(\sum_{t=1}^{r} w_i^S \times X^i + b_S\right) \tag{5}$$

where F is the activation function, b is a trainable bias parameter, and $w_i^s \times X^i$ is a two-dimensional discrete convolution operator [23]. The common activation function used with CNN is the rectified linear unit (ReLU).

The layer for pooling (pool) is the max-pooling layer determining the maximum value of a local patch (2 × 2 or 3 × 3) of the convolutional feature map output units. The process of max pooling is shown as:

$$Y_{j,k}^i = \max_{0 \le m,n<s}\left(X_{j,s+m,k,s+n}\right) \tag{6}$$

The $Y_{j,k}^i$ which is computed over a (s × s) non-overlapped local area in the (*ith*) input map, represents a neuron in the (*ith*) output activation map.

A fully connected (FC) layer, similar to a neural network, is the output of the last pooling or convolutional layers fed into fully connected layers (FC). The final layer of a CNN, known as the "Softmax layer," is used to categorize the features that were retrieved from earlier layers into N classes. The class membership probabilities are frequently output, transforming logit numbers into summative probabilities. The softmax operation can be computed, as shown in:

$$\text{softmax}(Y_i) = \frac{e^{y_i}}{\sum j^{e^{y_i}}} \tag{7}$$

3. Proposed Iris Recognition Scheme

This section proposes an IR scheme that aims to address the aforementioned issues and achieve high recognition accuracy, benefiting from the methods that were explained earlier. The proposed scheme entails two phases. The first phase is to propose a segmentation algorithm including four steps. The second phase is to propose an IR method. The proposed scheme is enumerated in the following sections:

3.1. Iris segmentation algorithm

In this study, a state-of-the-art iris segmentation algorithm has been proposed to address vibration and occlusion from the lashes and extract the ROI of the iris image. The segmentation algorithm has various steps which are shown in Fig. 2 and explained in the following sentences.

```
Variables:
   M: median filter
   H: histogram
   En: entropy
   Th: threshold value
   E max = max value entropy
   S = scale factor

Input: gray iris image Gray [i, j]
Start
   //Step 1 Process Middle filter
For i = 1, i < length of matrix image, i++
For j = 1, j < length of matrix image, j++
M Gray [i, j] Med ← gray [i, j]
end for
end for
   //Step 2 Process histogram
For i = 1, i < length of matrix image, i++
For j = 1, j < length of matrix image, j++
HiGray [Gray [i, j]] ← gray [i, j]
end for
end for
   //Step 3 Process entropy function
For i = 1, i < length of matrix image, i++
For j = 1, j < length of matrix image, j++
En Gray [i, j] ← Eq. (3)
Emax ← En Gray [i, j]
   //Step 4 Process binarization
For i = 1, i < length of matrix image, i++
For j = 1, j < length of matrix image, j++
If (i <= E max) then HiGray [i, j] = 0;
   else HiGray [i, j] = 255;
end for
end for
Binary [i, j] ← HiGray [0, 255]
   //Step 5 Process dilation
For i = 1, i < length of matrix image, i++
For j = 1, j < length of matrix image, j++
Dilation [i, j] ← [Binary [i, j] × S]
ROI [i, j] ← Dilation [i-i_i, j-j_j]
end for
end for
   //Step 6 Transform to gray
Gray [i, j] ← ROI [i, j]
```

Fig. 2 Proposed iris segmentation algorithm

(1) Determine the image histogram: First, capture an iris image and transform it to a grayscale. Then, utilizing Eq. (1), compute the histogram to determine the distribution of pixel intensities in the image. The x-axis of the histogram represents the intensity levels (0-255), while the frequency of each intensity is shown on the y-axis. Fig. 3 displays a sample histogram for a single iris image.

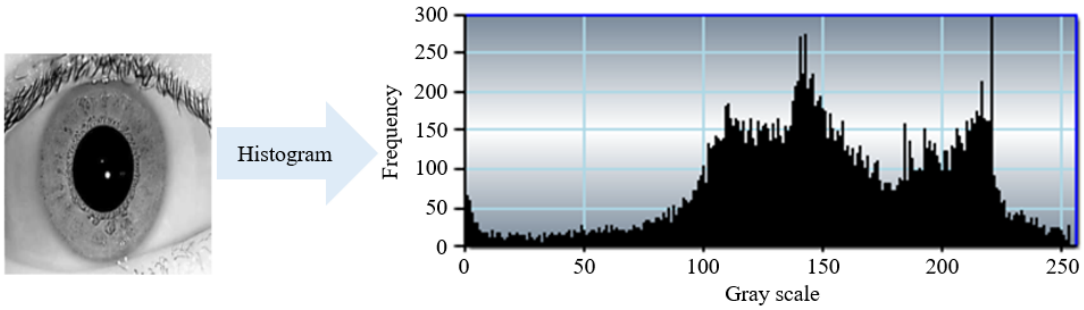

Fig. 3 Representation of original and histogram image

(2) Apply median filter for gray image. Fig. 4 shows an example of an iris image after applying a median filter.

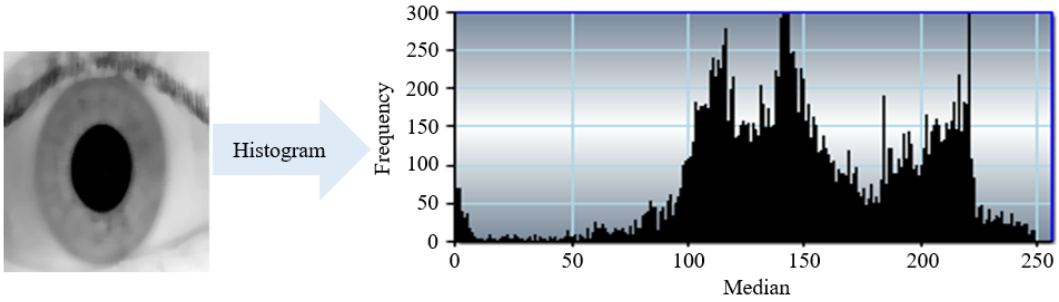

Fig. 4 Representation of original and filtered Image with a histogram-based median filter

(3) Maximum entropy value: First, determine the grayscale image's probability distribution for the pixel intensities. Then, use the entropy formula, i.e., Eq (3), to find the entropy image. Finally, output the maximum value of entropy after calculating the entropy values, and subsequently, determine the maximum entropy value. Table 2 provides an example of the maximum entropy for an image.

Table 2 Maximum entropy for an iris image

Max entropy value	Location (ppt)	Time (sec)
8.86030148358909	97	00:00:00.0428876

The maximum entropy value has been used as an adaptive threshold for the image. The threshold value is compared with all the intensities in the histogram. If the intensity value is larger than the threshold value, the intensity will be 1, and, in contrast, if it's smaller than the threshold, it will be 0. The result is a binary image will be used in the next step. According to Fig. 5, the filtered image is converted from gray to binary level by utilizing the maximum entropy value as a threshold.

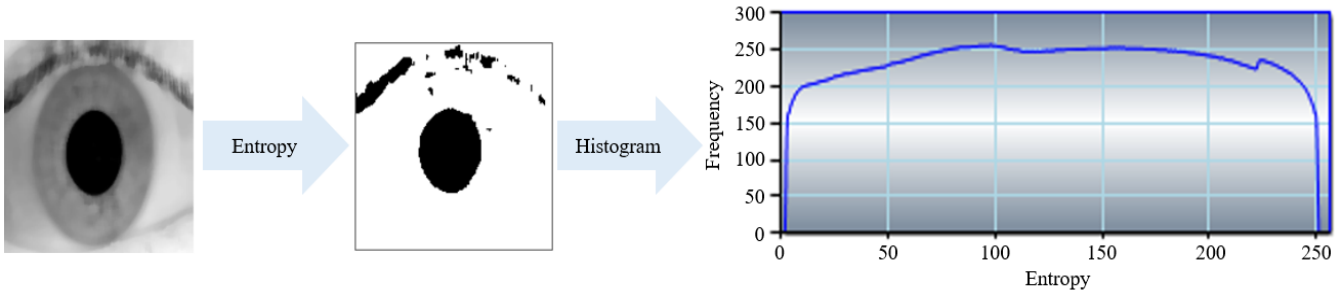

Fig. 5 Conversion from filtered to binary image via maximum entropy threshold

(4) Apply dilation morphology: Use the dilation morphology on the binary image obtained in Step 1 to extract the ROI of the iris, which includes the iris and its content. The dilated image is black and white, where the black areas represent the objects, and the white areas serve as the background. To distinguish the iris region from the undesirable area of the images, four regions have been defined according to the proposed algorithm, as depicted in Fig. 6. Moreover, the regions are based on the computation of white and black points in each row and column in all four regions. Finally, besides, the drawn rectangle region is the result.

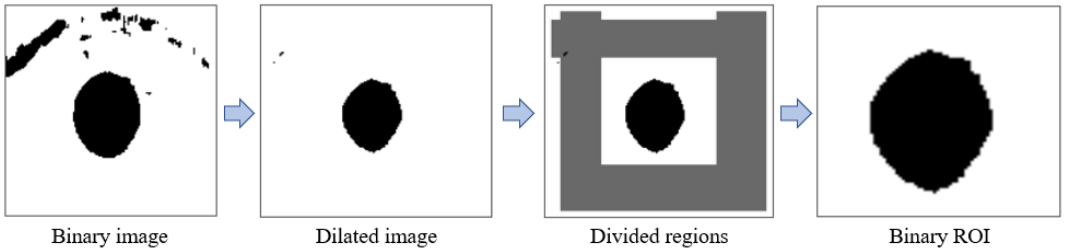

Fig. 6 Iris region segmentation with the proposed algorithm

(5) Transform to a gray image and convert the ROI binary to gray, as shown in Fig. 7.

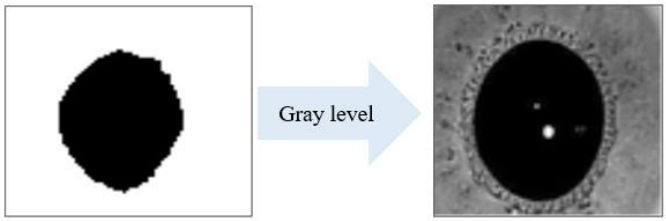

Fig. 7 Transformation of binary ROI to gray ROI

3.2. Iris recognition scheme

IR is the second phase in the proposed scheme, and the ROI iris images are fed into the recognition step using CNN. CNNs use convolutional and pooling layers to automatically extract information from the ROI iris images. Meanwhile, specifically, the features are the borders of iris, texture patterns, etc.

The CNN requires itself to be trained on a dataset of labeled iris images before being used for recognition. The network learns to map the input ROI iris images with matching iris identities during training. CNN can recognize iris images if having been trained. The stage herein involves feeding the trained CNN with the ROI iris images. By using softmax activation in the output layer for classification tasks, the network subsequently outputs a probability distribution over sundry identities of the iris. Typically, the most probable identity is selected to be the recognized identity.

To evaluate whether the performance of a CNN-based IR system is effective, the recognition metrics such as accuracy and receiver operating characteristic (ROC) curves are deployed. Diagrammatically, Fig. 8 illustrates the CNN representation.

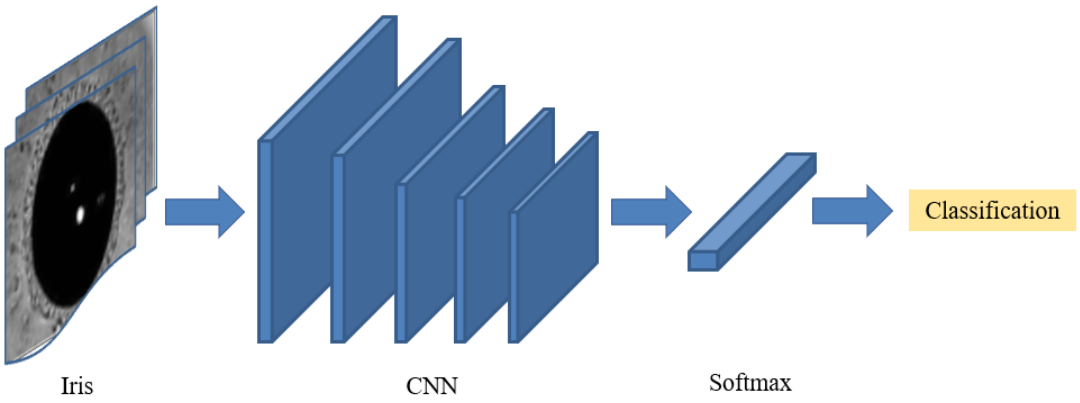

Fig. 8 CNN representation

4. Experimental Results

Regarding the results, a scheme has been developed with multiple functions. The pre-processing step is applied initially, and afterward, the images are binarized. Furthermore, the segmented images are recognized using the CNN classifier. In the recognition step, the accuracy rate, which is determined by the confusion matrix, is used as the criterion to assess the performance of the recommended scheme. The analysis is implemented using the Windows 10 algorithms in C# (Microsoft Visual Studio 2013).

4.1. Database

In this study, the IIT Delhi iris images database version 1.0 is utilized [24]. The majority of the iris scans in this database were taken from the students of the Indian Institute of Technology, Delhi, and personnel in India. The database was compiled using JIRIS, JPC1000, and CMOS camera, in the Biometrics Research Laboratory from January to July 2007. The

photos captured were stored in bitmap format. 2,240 photos in the database were collected from 224 individuals and rendered freely available to the researchers. The participants account for 176 men and 48 women who are all between the ages of 14 and 55.

All of the images in this collection have a resolution of 320 by 240 pixels and were all taken indoors. All of the photographs in the database yielded from unpaid volunteers who received no payment or honoraria. Participants must present their eyes sequentially until ten photos are registered for the images to be captured using an automated program. To examine the proposed scheme, every image in the database has been used. Samples from the IIT Delhi dataset are shown in Fig. 9.

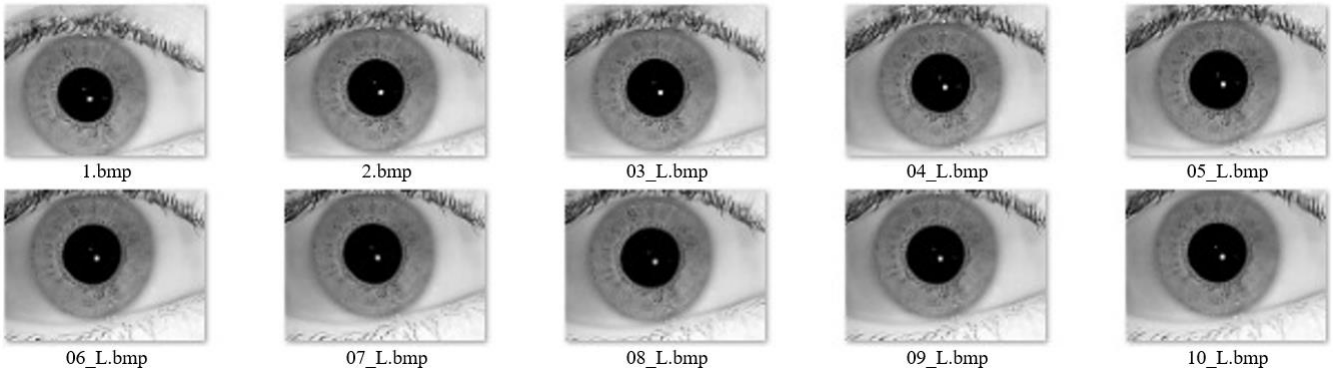

Fig. 9 Samples of the IIT Delhi dataset

4.2. Result-based segmentation

Fig. 10 presents samples of correct iris image segmentation scheme steps using the proposed algorithm. However, the segmentation stage was hindered because of differences in iris images and occlusions of the eyelashes and lids incurring incorrect segmentation, as shown in Fig. 11.

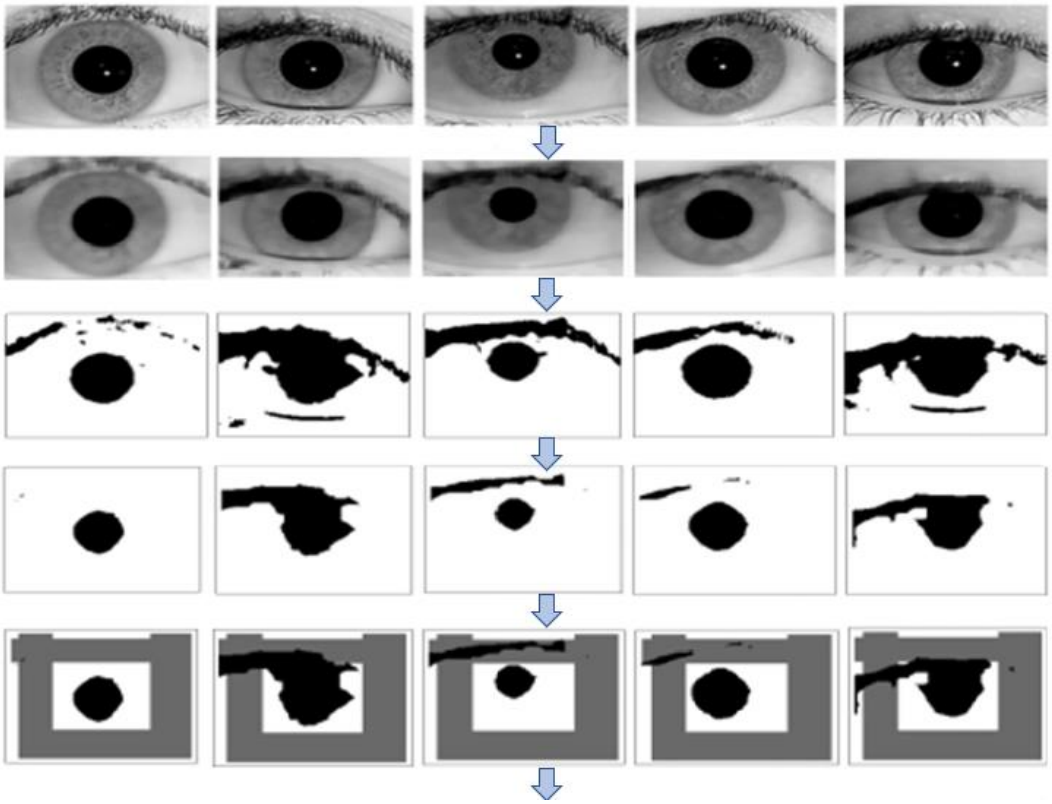

Fig. 10 Iris image segmentation steps using the proposed algorithm

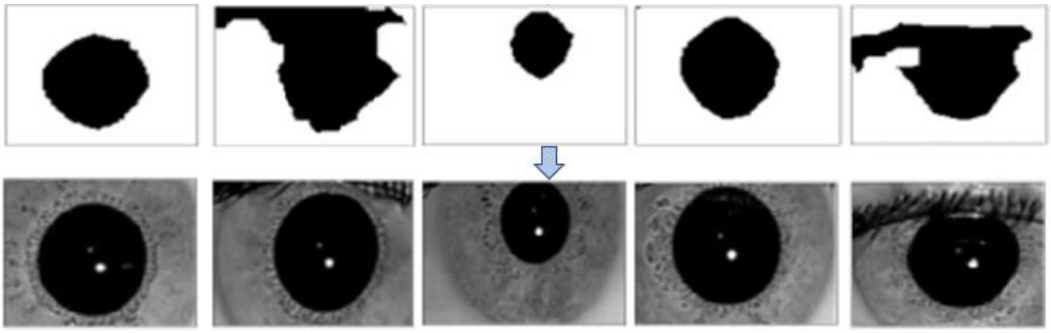

Fig. 10 Iris image segmentation steps using the proposed algorithm (continued)

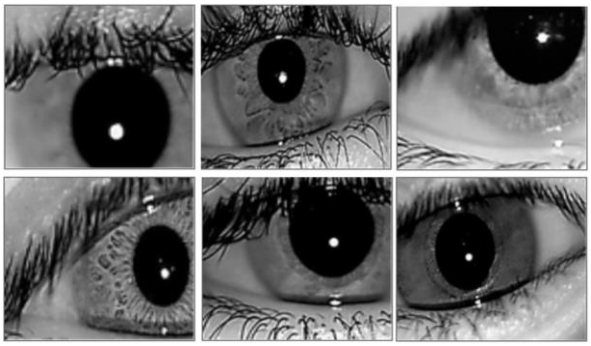

Fig. 11 Samples of incorrect image segmentation

To perform the computations and evaluate the flawed cropping manually, the accuracy can be determined based on [25-26] using the formula below.

$$Accurcy = \frac{corect_{image}}{all_{image}} \tag{8}$$

Based on Eq. (8), the accuracy of the proposed scheme reaches 93%.

4.3. Results-based recognition

The structure of the proposed CNN consists of two convo layers, two pool layers, one for each FC, and a softmax layer. The rate of learning is 0.0001. In addition, the standard stride size having been applied is equal to 1. Two experiments are conducted. The first experiment uses half of the dataset's images, and the second uses all of the images. The dataset used is categorized into 80% training and 20% testing. Moreover, the pre-trained AlexNet model has been employed to extract features. The accuracy rate of ratio recognition varies with the number of epochs, as shown in Fig. 12.

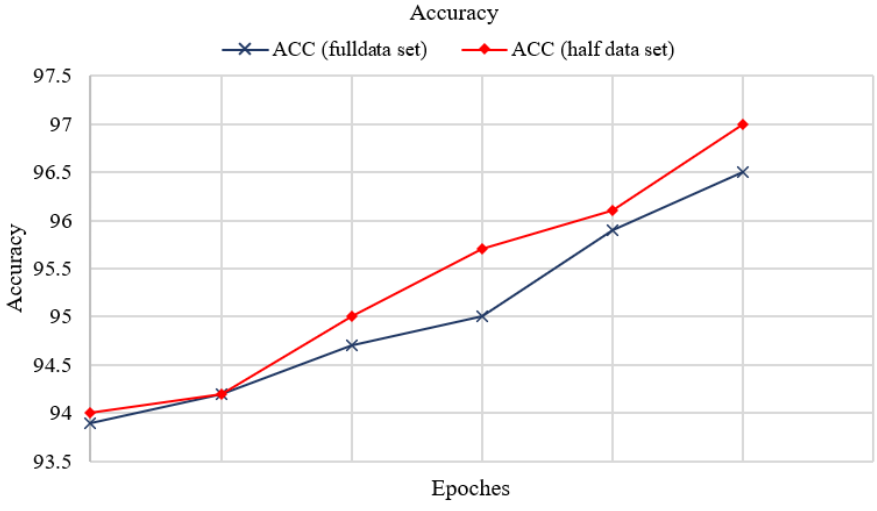

Fig. 12 Accuracy recognition rate

Specifically, Fig. 12 indicates the number of epochs is directly proportional to the performance. As a result, five epochs were considered in the final implementation. The recognition model outperforms smaller datasets due to growing excessively intricate and recording noises or random fluctuations in the data while working with similar image datasets. Therefore, the accuracy reaches 97.5% when using the full dataset. On the other hand, the optimal accuracy reaches 98.8% when using half of the dataset. Furthermore, Fig.13 illustrates ROC curves depicting the performance characteristics and demonstrating the accuracy of IR results.

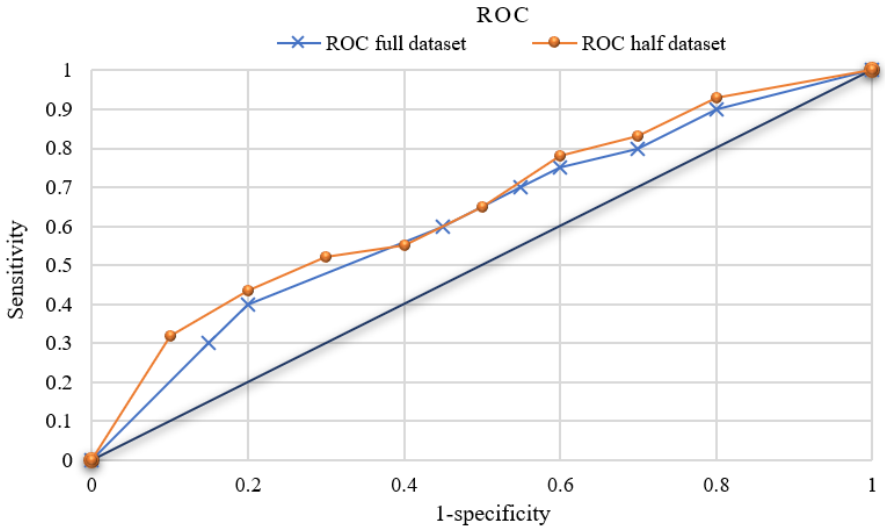

Fig. 13 ROC curve

5. Conclusion

In this study, two phases emerge to the proposed scheme, i.e., the segmentation method as the first phase and the IR technique based on CNN as the second phase. A major component of IR systems is iris segmentation algorithms. Any biometric authentication system includes the segmentation step for improved recognition. The suggested scheme aims to identify an appropriate segmentation for images of the iris. These images include manifold locations, hindering the accessibility to determine the ideal ROI. The proposed method uses the 2D histogram entropy during the binarization. Morphological dilation is used to extract the ROI while increasing the image's level of detail. The results are regarded as the missing-cropped ROI when the images are noticeably misaligned. The accuracy of the segmentation stands at approximately 93%. Additionally, in the recognition phase, the accuracy reaches 98.8% using half of the dataset. Meanwhile, the accuracy stands at 97.5% using the full dataset. ROC curves show the accuracy of the findings of iris identification and illustrate the performance characteristics. Concerning future work, the proposed iris scheme is envisaged to be used on another dataset.

Conflicts of Interest

The authors declare no conflict of interest.

Statement of Ethical Approval

All procedures performed in studies involving human participants were in accordance with the ethical standards of the institutional and/or national research committee and with the 1964 Helsinki declaration and its later amendments or comparable ethical standards.

Statement of Informed Consent

For this type of study, informed consent is not required.

References

[1] I. S. Hussein, S. B. Sahibuddin, M. J. Nordin, and N. N. B. A. Sjarif, "Multimodal Recognition System Based on High-Resolution Palmprints," IEEE Access, vol. 8, pp. 56113-56123, 2020.

[2] G. Huo, D. Lin, and M. Yuan, "Multi-Source Heterogeneous Iris Segmentation Method Based on Lightweight Convolutional Neural Network," IET Image Processing, vol. 17, no. 1, pp. 118-131, January 2023.

[3] S. K. Balasubramanian, V. Jeganathan, and T. Subramani, "Deep Learning-Based Iris Segmentation Algorithm for Effective Iris Recognition System," Proceedings of Engineering and Technology Innovation, vol. 23, pp. 60-70, January 2023.

[4] M. Mostofa, S. Mohamadi, J. Dawson, and N. M. Nasrabadi, "Deep Gan-Based Cross-Spectral Cross-Resolution Iris Recognition," IEEE Transactions on Biometrics, Behavior, and Identity Science, vol. 3, no. 4, pp. 443-463, October 2021.

[5] J. G. Daugman, "High Confidence Visual Recognition of Persons by a Test of Statistical Independence," IEEE Transactions on Pattern Analysis and Machine Intelligence, vol. 15, no. 11, pp. 1148-1161, November 1993.

[6] J. Daugman, "How Iris Recognition Works," The Essential Guide to Image Processing, 2nd ed., Amsterdam: Academic Press, pp. 715-739, 2009.

[7] C. S. Hsiao, C. P. Fan, and Y. T. Hwang, "Design and Analysis of Deep-Learning Based Iris Recognition Technologies by Combination of U-Net and EfficientNet," 9th International Conference on Information and Education Technology, pp. 433-437, March 2021.

[8] X. Nie, H. Wang, B. Chai, and M. Duan, "Remote Sensing Image Instance Segmentation Based on Attention Balanced Feature Pyramid," International Journal of Pattern Recognition and Artificial Intelligence, vol. 37, no. 1, article no. 2254020, January 2023.

[9] H. D. Rafik and M. Boubaker, "Application of Metaheuristic for Optimization of Iris Image Segmentation by Using Evaluation Hough Transform and Methods Daugman," 1st International Conference on Communications, Control Systems and Signal Processing, pp. 142-150, May 2020.

[10] S. Rapaka, P. Rajesh Kumar, M. Katta, K. Lakshminarayana, and N. Bhupesh Kumar, "A New Segmentation Method for Non-Ideal Iris Images Using Morphological Reconstruction FCM Based on Improved DSA," SN Applied Sciences, vol. 3, no. 1, article no. 53, January 2021.

[11] B. K. O. C. Alwawi and A. F. Y. Althabhawee, "Towards More Accurate and Efficient Human Iris Recognition Model Using Deep Learning Technology," TELKOMNIKA Telecommunication Computing Electronics and Control, vol. 20, no. 4, pp. 817-824, August 2022.

[12] M. Omran and E. N. AlShemmary, "An Iris Recognition System Using Deep Convolutional Neural Network," Journal of Physics: Conference Series, vol. 1530, article no. 012159, 2020.

[13] M. G. Alaslani and L. A. Elrefaei, "Convolutional Neural Network Based Feature Extraction for IRIS Recognition," International Journal of Computer Science & Information Technology, vol. 10, no. 2, pp. 65-78, April 2018.

[14] S. Minaee and A. Abdolrashidi, "Deepiris: Iris Recognition Using a Deep Learning Approach," https://doi.org/10.48550/arXiv.1907.09380, July 22, 2019.

[15] Z. Wang, C. Li, H. Shao, and J. Sun, "Eye Recognition with Mixed Convolutional and Residual Network (MiCoRe-Net)," IEEE Access, vol. 6, pp. 17905-17912, 2018.

[16] M. S. Azam and H. K. Rana, "Iris Recognition Using Convolutional Neural Network," International Journal of Computer Applications, vol. 175, no. 12, pp. 24-28, August 2020.

[17] S. K. Tummala and I. Priyadarshini T, "Morphological Operations and Histogram Analysis of SEM Images Using Python," Indian Journal of Engineering and Materials Sciences, vol. 29, no. 6, pp. 796-800, December 2022.

[18] I. S. Hussein, S. B. Sahibuddin, M. J. Nordin, and N. N. Amir, "The Extract Region of Interest in High-Resolution Palmprint Using 2D Image Histogram Entropy Function," Journal of Computer Science, vol. 15, no. 5, pp. 635-647, 2019.

[19] R. Hermary, G. Tochon, É. Puybareau, A. Kirszenberg, and J. Angulo, "Learning Grayscale Mathematical Morphology with Smooth Morphological Layers," Journal of Mathematical Imaging and Vision, vol. 64, no. 7, pp. 736-753, September 2022.

[20] P. Kim, MATLAB Deep Learning: With Machine Learning, Neural Networks and Artificial Intelligence, New York: Apress, pp. 121-147, 2017.

[21] B. Moons, D. Bankman, and M. Verhelst, Embedded Deep Learning: Algorithms, Architectures and Circuits for Always-on Neural Network Processing, Cham: Springer, 2019.

[22] A. F. Gad, Practical Computer Vision Applications Using Deep Learning with CNNs, 1st ed., Berkley: Apress, 2018.
[23] S. Minaee, A. Abdolrashidiy, and Y. Wang, "An Experimental Study of Deep Convolutional Features for Iris Recognition," IEEE Signal Processing in Medicine and Biology Symposium, pp. 1-6, December 2016.
[24] A. K. Pathak and A. Passi, "Comparison and Combination of Iris Matchers for Reliable Personal Identification," IEEE Computer Society Conference on Computer Vision and Pattern Recognition Workshops, article no. 4563110, June 2008.
[25] T. H. Mandeel, M. I. Ahmad, M. N. Md Isa, S. A. Anwar, and R. Ngadiran, "Palmprint Region of Interest Cropping Based on Moore-Neighbor Tracing Algorithm," Sensing and Imaging, vol. 19, no. 1, article no. 15, December 2018.
[26] I. S. Hussein and N. N. A. Sjarif, "Human Recognition Based on Multi-Instance Ear Scheme," International Journal of Computing, vol. 22, no. 3, pp. 397-403, October 2023.